EBioMedicine 43 (2019) 225–237

Contents lists available at ScienceDirect

EBioMedicine

journal homepage: www.ebiomedicine.com

EBioMedicine
Published by THE LANCET

Research paper

# MYC status as a determinant of synergistic response to Olaparib and Palbociclib in ovarian cancer

Jingyan Yi [a,1], Chongya Liu [a,1], Zhiwei Tao [a], Min Wang [a], Yaxun Jia [a], Xiaolin Sang [a], Lanlin Shen [a], Yijue Xue [a], Kui Jiang [b], Fuwen Luo [c], Pixu Liu [a,d,**], Hailing Cheng [a,*]

[a] Cancer Institute, The Second Hospital of Dalian Medical University, Institute of Cancer Stem Cell, Dalian Medical University, Dalian 116044, China
[b] Department of Oncology, The Second Hospital of Dalian Medical University, Dalian 116044, China
[c] Department of Acute Abdomen Surgery, The Second Hospital of Dalian Medical University, Dalian 116044, China
[d] College of Pharmacy, Dalian Medical University, Dalian 116044, China

ARTICLE INFO

*Article history:*
Received 11 November 2018
Received in revised form 11 March 2019
Accepted 11 March 2019
Available online 18 March 2019

*Keywords:*
MYC
PARP inhibitor
CDK4/6 inhibitor
HR repair
Ovarian cancer

ABSTRACT

*Background:* While PARP inhibitors and CDK4/6 inhibitors, the two classes of FDA-approved agents, have shown promising clinical benefits, there is an urgent need to develop new therapeutic strategies to improve clinical response. Meanwhile, extending the utility of these inhibitors beyond their respective molecularly defined cancer types is challenging and will likely require biomarkers predictive of treatment response especially when used in a combination drug development setting.
*Methods:* The effects of PARP inhibitor Olaparib and CDK4/6 inhibitor Palbociclib on ovarian cancer cells lines including those of high-grade serous histology were examined *in vitro* and *in vivo*. We investigated the molecular mechanism underlying the synergistic effects of drug combination.
*Findings:* We show for the first time that combining PARP and CDK4/6 inhibition has synergistic effects against MYC overexpressing ovarian cancer cells both *in vitro* and *in vivo*. Mechanistically, we find that Palbociclib induces homologous recombination (HR) deficiency through downregulation of MYC-regulated HR pathway genes, causing synthetic lethality with Olaparib. We further demonstrate that MYC expression determines sensitivity to combinatorial treatment with Olaparib and Palbociclib.
*Interpretation:* Our data provide a rationale for clinical evaluation of therapeutic synergy of these two classes of inhibitors in ovarian cancer patients whose tumors show high MYC expression and who do not respond to PARP inhibitors or CDK4/6 inhibitors monotherapies.
*Fund:* This work was supported by the National Natural Science Foundation of China [81672575, 81874111, 81472447 to HC; 81572586 and 81372853 to PL], and the Liaoning Provincial Key Basic Research Program for Universities [LZ2017002 to HC].


## 1. Introduction

Ovarian cancer is one of the deadliest gynecological diseases, accounting for over 140,000 deaths annually worldwide [1–3]. Despite initial high response rates to cytoreductive surgery followed by platinum-taxane chemotherapy, >70% of these patients will relapse with limited subsequent treatment options [4,5]. Three PARP inhibitors (PARPi), Olaparib, Rucaparib and Niraparib, have been approved by the FDA for the treatment of recurrent ovarian cancers [6]. The clinical use of this class of drugs has the potential to favorably change the treatment outcomes of gynecological malignancies. Approximately 50% of epithelial ovarian cancers exhibit defective DNA repair *via* homologous recombination (HR) [7,8]. PARP inhibitors exploit the fundamental vulnerability of ovarian cancer with homologous recombination repair deficiency and have showed promising anti-tumor effect on ovarian cancers with deleterious *BRCA1/2* mutations or BRCAness [5,6,9–12]. Increasing evidence also indicates the efficacy of PARP inhibitors in ovarian cancers in the absence of *BRCA1/2* mutations, presumably resulting from other molecular deficiencies in HR repair [13–15]. Indeed, emerging novel combination therapeutic strategies designed to selectively

* Corresponding author at: Cancer Institute, Dalian Key Laboratory of Molecular Targeted Cancer Therapy, The Second Hospital of Dalian Medical University, Dalian, Liaoning, China.
** Corresponding author at: Institute of Cancer Stem Cell, College of Pharmacy, Dalian Medical University, Dalian, Liaoning, China
*E-mail addresses:* pixu_liu@dmu.edu.cn (P. Liu), hailingcheng_dmu@163.com (H. Cheng).
[1] These authors contributed equally to this work

https://doi.org/10.1016/j.ebiom.2019.03.027

**Research in context**

*Evidence before this study*

FDA has approved three PARP inhibitors and three CDK4/6 inhibitors in recent years, for recurrent ovarian cancer and advanced ER-positive breast cancer, respectively. A large number of early-stage clinical trials examining PARPi-based or CDK4/6i-based combination therapies are currently under way in a variety of human malignancies including ovarian cancer. However, none of these trials involves a combination of these two classes of inhibitors, likely due to a lack of reliable biomarkers that are predictive of therapeutic response.

*Added value of this study*

We demonstrate the therapeutic synergy between PARP and CDK4/6 inhibition and identify MYC status as a determinant of sensitivity to combined use of Olaparib and Palbociclib in ovarian cancer cell lines including those with high-grade serous histology.

*Implications of all the available evidence*

Our finding of MYC-dependent therapeutic synergy between PARP and CDK4/6 inhibitors may warrant clinical assessment with a potential to benefit ovarian cancer patients whose tumors harbor MYC amplification and/or overexpression.

disrupt HR repair in cancer cells and render vulnerabilities to PARP inhibitors have been evaluated preclinically and in early clinical trials of a variety of cancer types including ovarian cancer [6,9,10].

Inhibitors of cyclin-dependent kinases 4/6 (CDK4/6) have emerged as a powerful class of agents for cancer treatment [16]. When used in combination with endocrine therapy, CDK4/6 inhibitors have promising clinical activity in metastatic estrogen receptor-positive ($ER^+$), HER2-negative ($HER2^-$) breast cancers [16,17]. Blocking CDK4/6 will lead to the suppression of retinoblastoma protein (RB) phosphorylation and concomitant inhibition of G1-S cell-cycle progression through repressing E2F-mediated transcription [18]. Additional CDK4/6 inhibitor based-combination treatments have been studied in preclinical models of multiple tumor types, many of which are now the subject of ongoing clinical trials (*www.clinicaltrials.gov*), including those in combination with chemotherapy in $ER^+/HER2^-$ breast cancer, with T-DM1 in $HER2^+$ breast cancer, with androgen antagonists (*e.g.* enzalutamide) in prostate cancer, with MEK inhibitors in melanoma and with ibrutinib in mantle cell lymphoma.

While PARPi and CDK4/6i, both classes of agents, have shown promising clinical benefits, extending the utility of these inhibitors beyond their respective molecularly defined cancers to circumvent intrinsic or acquired drug resistance is quite challenging and will likely require predictive biomarkers of treatment response especially when used in combination [6,19]. In the current study, we investigated the efficacy of the combination of PARP inhibitor Olaparib and CDK4/6 inhibitor Palbociclib against ovarian cancer.

## 2. Materials and methods

### 2.1. Cell culture and reagents

PA-1 (#CRL-1572, RRID: CVCL_0479), CAOV3 (#HTB-75, RRID: CVCL_0201), SKOV3 (#HTB-77, RRID: CVCL_0532) human ovarian cancer cell lines were purchased from ATCC (Manassas, USA). SNU119 (#HTX2624, RRID: CVCL_5014) and COV362 (#HTX3065, RRID: CVCL_2420) human ovarian cancer cell lines were purchased from Otwo Biotech (China). IGROV1, OVCA433, HEYA8, OVCAR5, EFO27, OVCAR8, and A2780 human ovarian cancer cell lines were obtained from Dr. Jean Zhao at Dana-Farber Cancer Institute, Harvard Medical School. Cells were maintained in culture media (OVCA433, PA-1, SKOV3, HEYA8, CAOV3, OVCAR5, EFO27, and OVCAR8 cells in Dulbecco's Modified Eagle Medium; A2780, IGROV1, SNU119, and COV362 cells in RPMI-1640 Medium) supplemented with 10% fetal bovine serum and penicillin/streptomycin (100 units/ml) at 37 °C and 5% $CO_2$. Olaparib (AZD2281) and Palbociclib (PD-0332991) were purchased from Chemexpress (China).

### 2.2. Cell viability assay and determination of drug synergy

Cell viability was assayed using the cell counting kit-8 assay according to the manufacturer's protocol (Dojindo Molecular Technologies, Japan). Synergistic effects were determined by the Chou-Talalay method to calculate the combination index (CI) [20].

### 2.3. Clonogenic assay

Cells were seeded on plates and cultured for 24 h before the initiation of drug treatment. Fresh media containing drugs were replaced every 3 days. At the end point, cells were washed with phosphate buffered solution and subsequently stained with 5% crystal violet for 1 h. Images of stained plates were captured using Molecular Imager (USA). The optical absorbance of bound crystal violet (dissolved in 50% acetic acid) was measured at 570 nm by Multi-functional microplate reader Enspire230 (Perkin Elmer, USA).

### 2.4. Three-dimensional sphere assay

Three-dimensional sphere culture experiments were performed as previously described [21]. Cells were seeded on plates with 50% precoated matrigel (BD Biosciences, USA) plus 50% of medium without serum. Culture medium supplemented with 5% fetal bovine serum and 2% matrigel was replaced every 3 days. Three-dimensional culture experiments were imaged by inverted phase contrast microscope (Leica Microsystems, Germany) and scored according to 3D structure integrity. Over 100 structures were scored for each type of drug treatment.

### 2.5. Western blot analysis

Cells were harvested in RIPA lysis buffer containing a proteinase cocktail (Thermo Scientific, USA). Cell lysates were then analyzed by western blot. Antibodies against Cleaved-PARP (#5625, RRID: AB_10699459), MYC (#5605, RRID: AB_1903938) and phosphorylated Rb (Serine 807/811) (#8516, RRID: AB_11178658) were from Cell Signaling Technology (USA). Vinculin (#V9131, RRID: AB_477629) was from Sigma-Aldrich (USA). Immunofluorescently labeled secondary antibodies to rabbit-IgG (Molecular Probes, USA) or mouse-IgG (Rockland Immunochemicals, USA) were used. Western blots were imaged with Odyssey (LI-COR Biosciences, USA). MYC protein abundance was quantified using Image Studio software (LI-COR Biosciences) and normalized to Vinculin.

### 2.6. Flow cytometry analysis

Apoptosis in ovarian cancer cells was analyzed with Annexin V-FITC Apoptosis Detection Kit (Dojindo Molecular Technologies, Japan) according to manufacturer's instructions. Briefly, cultured cells were trypsinized with 0.25% trypsin without EDTA, and then stained with Annexin V-FITC and Propidium iodide (PI) solution. Stained cells were subjected to flow cytometry analysis on BD FACS Aria II (BD Biosciences, USA).

### 2.7. RNA sequencing (RNA-Seq) analysis

RNAs isolated from A2780 cells were treated with DMSO, Olaparib, Palbociclib, and their combination (Ola/Palb) for 24 h. The RNA-Seq analysis was performed by Novogene (China). Sequencing libraries were generated using NEBNext® UltraTM RNA Library Prep Kit for Illumina® (NEB, USA) following manufacturer's recommendations. Heat map was drawn using individual genes from HR repair pathway with 'pheatmap' package. Parametric *t*-test *P* values and false discovery rate (FDR) values were reported for each gene. GSEA was performed by the JAVA program (http://software.broadinstitute.org/gsea/index.jsp) using MSigDB Hallmark and KEGG gene set collection. 1000 random sample permutations were carried out, and the significance threshold was set at $P$ value < 0.05 and nominal FDR < 0.05. The RNA-seq dataset was deposited to the Gene Expression Omnibus (GEO) with accession number GSE126998.

### 2.8. Quantitative reverse transcription-PCR analysis

RNA was extracted using Trizol (Life Technologies, USA). Reverse transcription reaction was performed using PrimeScript RT Master Mix kit (Takara, Japan). Quantitative PCR was performed using SYBR Green PCR Master Mix (Applied Biosystems, USA) on Mx3005P real-time PCR system (Aglient, USA). Gene expression was normalized to *ACTB*. The following primers were used:

*ACTB*
5′-CATGTACGTTGCTATCCAGGC-3′(Forward)
5′-CTCCTTAATGTCACGCACGAT-3′(Reverse)
*RAD51*
5′-GGTCTGGTGGTCTGTGTTGA-3′(Forward)
5′-GGTGAAGGAAAGGCCATGTA-3′(Reverse)
*BRCA1*
5′-GTCCCATCTGTCTGGAGTTGA-3′(Forward)
5′-AAAGGACACTGTGAAGGCCC-3′(Reverse)
*BRCA2*
5′-TGCCTGAAAACCAGATGACTATC-3′(Forward)
5′-AGGCCAGCAAACTTCCGTTTA-3′(Reverse)
*LDHA*
5′-ATGTTGCTGGTGTCTCTCTGAAG-3′(Forward)
5′-GCCCAGGATGTGTAGCCT-3′(Reverse)
*ODC1*
5′-AGCCATCGTGAAGACCCTTG-3′(Forward)
5′-TGCATAGATAATCCTCTCTGGAGGC-3′(Reverse)
*MYC*
5′-AGGGTCAAGTTGGACAGTGTCA-3′(Forward)
5′-TGGTCGATTTTCGGTTGTTG-3′(Reverse)

### 2.9. Immunofluorescence staining analysis

Cells were fixed with 4% formaldehyde in PBS after drug treatment, blocked using 5% BSA, and permeabilized with 0.1% Triton X-100. RAD51 (#ab133534, RRID: AB_2722613) antibody was from Abcam (UK). γH2AX (#2577, RRID: AB_2118010) antibody was from Cell Signaling Technology (USA). DAPI was from Sigma-Aldrich (USA). Fluorescent secondary antibodies were used and images were captured with a fluorescence microscope (Olympus, Japan).

### 2.10. Comet assay

A comet assay was performed as previously described [22]. 200 randomly selected cells were analyzed using Casplab software. The level of DNA damage was presented as percentage of DNA in tail. Images were captured with a fluorescence microscope (Olympus, Japan).

### 2.11. Metaphase chromosome spread assay

Cells were treated with colchicine (0.5 μg/ml) (Coolaber, China) for 6 h prior to harvest. Metaphase spreads were prepared as described previously [23]. Images were captured with a fluorescence microscope (Olympus, Japan).

### 2.12. siRNA and plasmids

The siRNA reagents were purchased from GenePharma (Suzhou, China). Lipofectamine 2000 (Invitrogen, USA) was used to transfect on-target (human *MYC*: 5′-GCTTGTACCTGCAGGATCT-3′) and negative control siNC into the cells according to the manufacturer's protocol. The retroviral vectors used in this study were MSCV PIG (Puro IRES GFP) (#18751, RRID: Addgene_18751) and pMSCVpuro-Flag-cMyc T58A (#20076, RRID: Addgene_20076).

### 2.13. Xenograft models and in vivo drug treatment studies

Eight-week-old female nude mice were purchased from Beijing Vital River Laboratory Animal Technology Co., Ltd. (China) and maintained in a pathogen-free environment. All animal procedures were conducted under the approval of the Animal Care and Use Committee of Dalian Medical University. Mice were inoculated subcutaneously with a mixture of $5 \times 10^5$ A2780 cells and matrigel per injection site. The drug treatment started when the tumor xenografts reached approximately 75 $mm^3$. Palbociclib was dissolved in 50 mM sodium lactate solution and administered *via* oral gavage at 125 mg/kg/day. Olaparib was dissolved in 10% hydroxypropyl-β-cyclodextrin for intraperitoneal administration and dosed at 50 mg/kg/day. Tumors were measured every other day with digital calipers and calculated using the following formula: tumor volume = $(\text{length} \times \text{width}^2)/2$.

### 2.14. Histological and Immunohistochemical staining analysis

Tumors were fixed in 10% buffered formalin overnight before paraffin embedding. Paraffin blocks were sectioned and stained with haematoxylin and eosin (H&E). The value for tumor cell density was calculated as the number of tumor cells per $mm^2$. For immunohistochemical staining analysis, antibodies against Cleaved-Caspase-3 (#9661, RRID: AB_2341188), γH2AX (#2577, RRID: AB_2118010), and phosphorylated Rb (Serine 807/811) (#8516, RRID: AB_11178658) were from Cell Signaling Technology (USA). Antibodies against Ki67 (#ab15580, RRID: AB_443209) and RAD51 (#ab133534, RRID: AB_2722613) were from Abcam (UK). Antibodies against MYC (#10828-1-AP, RRID: AB_2148585) was from Proteintech (USA). For each tumor sample, 3–5 random 40 × fields were scored. Digital images were submitted for quantitative image analysis using Image Pro-plus software.

### 2.15. Statistical analysis

Unpaired Student's *t*-test and one way ANOVA with Tukey's multiple-comparisons tests were performed using GraphPad Prism software for analysis of the data obtained *in vitro* and *in vivo*, respectively. $P$ value <0.05 was considered as statistical significance.

## 3. Results

### 3.1. Olaparib and Palbociclib synergize to inhibit the growth of a subset of ovarian cancer cells in vitro

To evaluate the effects of concomitant inhibition of PARP and CDK4/6, we assessed the response of a panel of ovarian cancer cell lines to Olaparib and Palbociclib as single-agents or in combination. Following 72-h drug treatment, the cytotoxic effects were determined by CCK-8

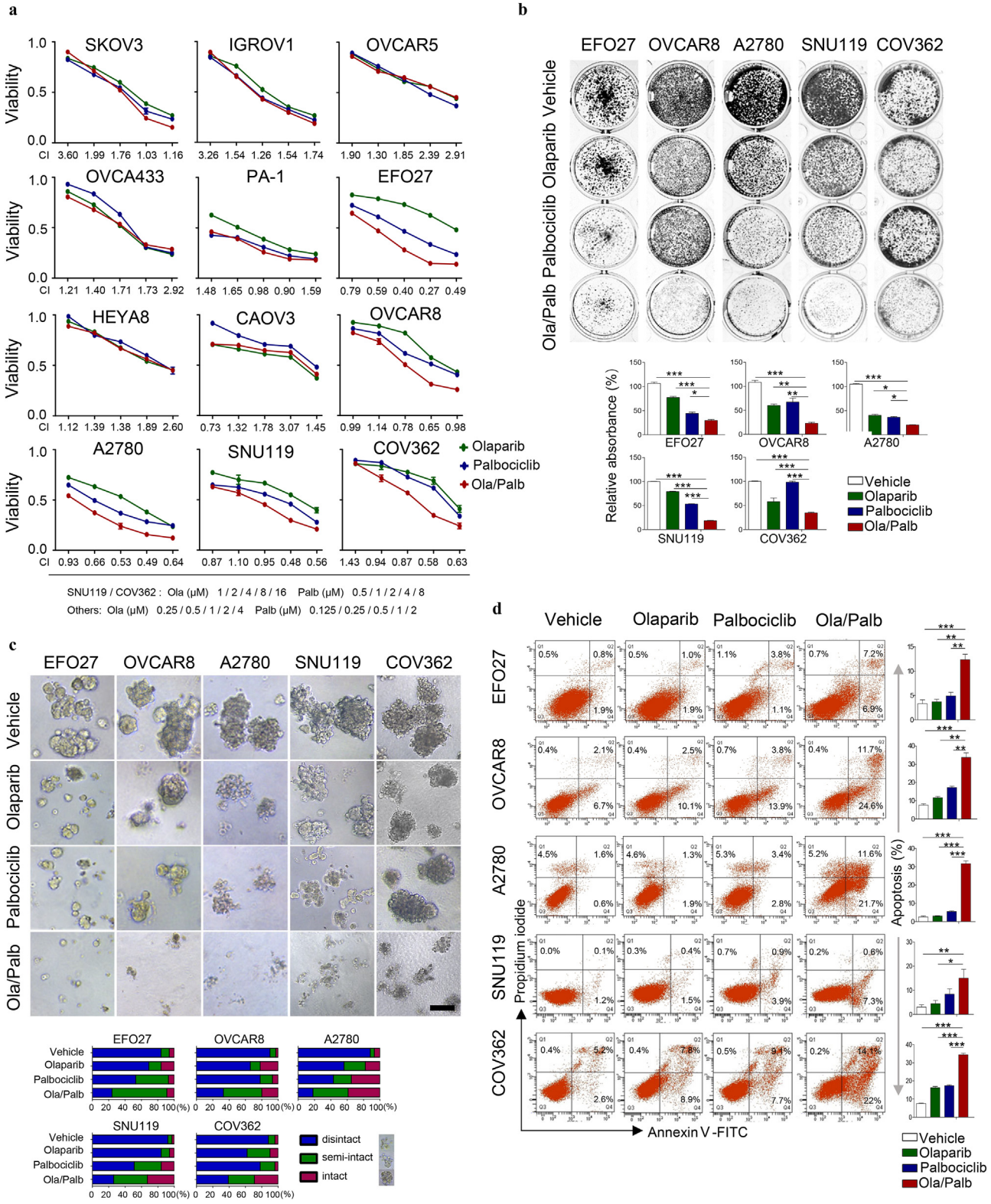


**Fig. 1.** Effects of Olaparib and Palbociclib as single-agents or in combination on the growth of ovarian cancer cell lines *in vitro*. (a) Dose-response curves of Olaparib or Palbociclib alone or combined in a panel of 12 ovarian cancer cell lines treated with varying concentrations of Olaparib and Palbociclib for 72 h. Combination index (CI) was calculated using CalcuSyn software with the Chou-Talalay equation. (b) EFO27, OVCAR8, A2780, SNU119, and COV362 ovarian cancer cell lines were treated with drugs for 7–10 days. Fresh medium with drugs was replaced every 3 days. At the end point, plates were fixed and stained with crystal violet stain. Representative images of plates are shown. Error bars represent standard deviations (S.D.) from the mean. EFO27, OVCAR8 and A2780: Olaparib (Ola), 2 μM; Palbociclib (Palb), 1 μM. SNU119 and COV362: Olaparib, 8 μM; Palbociclib, 4 μM. (c) Ovarian cancer cell lines were cultured in 3D matrigel and drug-treated for 10–15 days. Representative images of cells are shown. Quantification of scored structures (intact, semi-disintegrated and disintegrated) is shown. Scale bar, 200 μm. EFO27, OVCAR8, and A2780: Olaparib, 1 μM; Palbociclib, 0.5 μM. SNU119 and COV362: Olaparib, 4 μM; Palbociclib, 2 μM. (d) Ovarian cancer cell lines were drug-treated as indicated for 48 h. Flow cytometric analysis of Annexin V and propidium iodide (PI) stained cells was conducted to evaluate apoptosis. EFO27, OVCAR8 and A2780: Olaparib, 2 μM; Palbociclib, 1 μM. SNU119 and COV362: Olaparib, 8 μM; Palbociclib, 4 μM. Mean ± S.D. for three independent experiments are shown. $^{*}P < 0.05$; $^{**}P < 0.01$; $^{***}P < 0.001$ (Student's *t*-test).

assay followed by median-effect analysis. Of twelve ovarian cancer cell lines tested, five lines (EFO27, OVCAR8, A2780, SNU119, and COV362) demonstrated synergy as assessed by the CalcuSyn model (Fig. 1a and Supplementary Fig. 1). We further examined the synergistic growth inhibitory effects of the combination treatment in these cell lines by clonogenic survival assays. Compared to single-agents, combined use of Olaparib and Palbociclib induced a significantly stronger inhibitory effect on the growth of EFO27, OVCAR8, A2780, SNU119, and COV362 cells whereas similar observations were not seen in the other cell lines examined (Fig. 1b and Supplementary Fig. 2). Together, these data indicate that the combination of PARPi and CDK4/6i has synergistic activity against a subset of ovarian cancer cell lines.

To assess the drug effects in conditions that more closely mimic tumor microenvironment during cancer formation and progression *in vivo* [24], we subjected the five ovarian cancer cell lines (EFO27, OVCAR8, A2780, SNU119, and COV362) to culture as 3D spheroids in matrigel. While Olaparib and Palbociclib as single-agents each induced spheroid disintegration to a pronounced degree, the combination treatment led to a more substantial structural disintegration in all five ovarian cancer cell lines tested (Fig. 1c). Consistent with drug-induced therapeutic effect, combined use of Olaparib and Palbociclib but not either agent alone induced substantial apoptotic cell death as determined by flow cytometric Annexin V/PI measurement (Fig. 1d). Consistently, western blot analysis revealed a substantial increased abundance of cleaved PARP in cells treated with Olaparib and Palbociclib (Supplementary Fig. 3). These data provide further evidence for the synergistic effect of PARPi and CDK4/6i in ovarian cancer cells.

### 3.2. Palbociclib downregulates the expression of homologous recombination pathway genes, sensitizing ovarian cancer cells to PARP inhibition

The synergistic activity of PARPi and CDK4/6i prompted us to examine whether CDK4/6 inhibition may act in a synthetic lethal manner with PARP inhibition through inducing homologous recombination (HR) repair deficiency. For this, we assessed the effect of Palbociclib on the expression of HR repair pathway genes. Here we used A2780 cells, a combination treatment-responsive ovarian cancer cell line (Fig. 1), and subjected them to drug treatments followed by RNA-sequencing. Gene set enrichment analysis (GSEA) revealed a strong negative association of Palbociclib with E2F-target genes (Fig. 2a), thus consistent with the effect of CDK4/6 inhibition on repressing E2F-mediated transcription [18]. Further data analysis also identified a highly significant negative association between Palbociclib and HR repair pathway gene signature in A2780 ovarian cancer cells (Fig. 2a), with many HR repair pathway genes being strongly downregulated upon Palbociclib single-agent or in combination with Olaparib (Fig. 2b and Supplementary Fig. 4). Subsequent quantitative reverse transcription-PCR (qRT-PCR) analysis confirmed the remarkable downregulation of key HR repair pathway genes including *BRCA1*, *BRCA2* and *RAD51*, in A2780, EFO27, OVCAR8, SNU119, and COV362 ovarian cancer cells treated with Palbociclib (Fig. 2c). We also noticed a further downregulation of these genes in cells treated with Palbociclib and Olaparib in combination (Fig. 2c). The fact that CDK4/6 inhibition induces downregulation of HR repair genes prompted us to hypothesize that CDK4/6 inhibition by Palbociclib may induce HR repair deficiency and confer sensitivity to Olaparib in a synthetic lethal manner.

### 3.3. Palbociclib treatment results in HR deficiency, synergizing with Olaparib to induce DNA damage and genome instability

To test our hypothesis, we first explored a direct link between CDK4/6i- mediated inhibition of HR repair pathway gene expression and defective HR repair. Immunofluorescence staining analysis revealed that compared with vehicle, Palbociclib alone and, to a more significant extent in combination with Olaparib, reduced RAD51 nuclear foci (a marker for the competency of homologous recombination repair) but increased γH2AX nuclear foci (a surrogate marker for DNA double strand breaks, DSBs) (Fig. 3a). These results indicated that CDK4/6 inhibition may induce deficiency in homologous recombination repair of DSBs, a potential mechanism underlying synthetic lethality with PARP inhibition. We next examined whether CDK4/6i would increase PARPi-induced DNA damage by using a comet assay. Whereas Olaparib or Palbociclib modestly induced DNA damage, the combination treatment induced accumulation of damaged DNA (Fig. 3b). We also used a metaphase chromosome spread assay to assess the impact of combined PARPi and CDK4/6i on genome integrity. Compared with single-agents or vehicle, Olaparib and Palbociclib in combination induced significantly more aberrant chromosome structures (abnormal chromosome numbers, chromosome breaks and disjunction figures) (Fig. 3c), features of genomic instability. These results, together with the synergistic cytotoxicity data (Fig. 1), are consistent with the hypothesis that CDK4/6i is synthetic lethal with PARPi through inducing HR repair deficiency.

### 3.4. MYC expression determines synergistic response to combined PARPi and CDK4/6i

We next sought to investigate the molecular mechanism underlying the differential treatment responses to combined PARPi and CDK4/6i. Further gene set enrichment analysis of the RNA-seq data revealed a highly significant negative association between MYC target gene signature and Palbociclib alone or in combination with Olaparib in A2780 ovarian cancer cells, with many MYC targets being strongly downregulated upon drug treatments (Fig. 4a). Subsequent qRT-PCR analysis confirmed that the treatment with Palbociclib alone or in combination with Olaparib resulted in remarkable downregulation of well-described MYC transcriptional targets *LDHA* and *ODC1* [25,26] in the five PARPi-CDK4/6i responsive cell lines (A2780, EFO27, OVCAR8, SNU119, and COV362) (Fig. 4b). Concordantly, a substantial reduction of *MYC* protein abundance was detected in cells treated with Palbociclib alone or in combination with Olaparib (Supplementary Fig. 5). These results prompted us to examine the correlation of MYC expression levels with the treatment response to combined PARPi-CDK4/6i. To further look into this, we conducted western blot analysis of MYC protein abundance in the twelve ovarian cancer cell lines whose treatment response to combined use of Olaparib and Palbociclib was evaluated as shown in Fig. 1 and supplementary Fig. 1–2. We found that combination treatment-responsive cell lines (A2780, EFO27, OVCAR8, SNU119, and COV362) have significantly higher MYC protein levels than those non-responsive cell lines (Fig. 4c and Supplementary Fig. 6). Together, these data raised the possibility that MYC expression may determine treatment response to combined PARPi-CDK4/6i.

We next determined whether MYC influences tumor response to Olaparib and Palbociclib in combination. MYC knockdown abrogated the synergistic growth inhibitory effect on A2780, EFO27, OVCAR8, SNU119, and COV362 cells (Fig. 4d). Conversely, enforced expression of *MYC T58A*, a stabilized form of MYC [27], sensitized otherwise non-responsive IGROV1 and SKOV3 cells to combined PARPi-CDK4/6i and induced strong apoptotic cell death (Fig. 5a and b). Similarly, IGROV1 and SKOV3 cells with enforced expression of *MYC T58A* also exhibited significantly reduced expression of *BRCA1*, *BRCA2* and *RAD51*, increased accumulation of γH2AX foci (DNA double-strand break marker) and decreased RAD51 foci in response to CDK4/6 inhibition by Palbociclib single-agent and to a greater extent in combination with Olaparib (Fig. 5c and d). Notably, *MYC T58A* overexpression caused significantly increased *BRCA1* expression in both IGROV1 and SKOV3 cells, and also markedly increased expression of *BRCA2* and *RAD51* in IGROV1 but not SKOV3 cells (Supplementary Fig. 7). Comparable to the effects observed in ovarian cancer cells with high levels of endogenous MYC, Palbociclib alone or in combination with Olaparib also resulted in a significant reduction in the abundance of ectopically expressed MYC protein in IGROV1 and SKOV3 cells (Supplementary Fig. 8). Conversely, MYC knockdown resulted in significantly downregulated expression

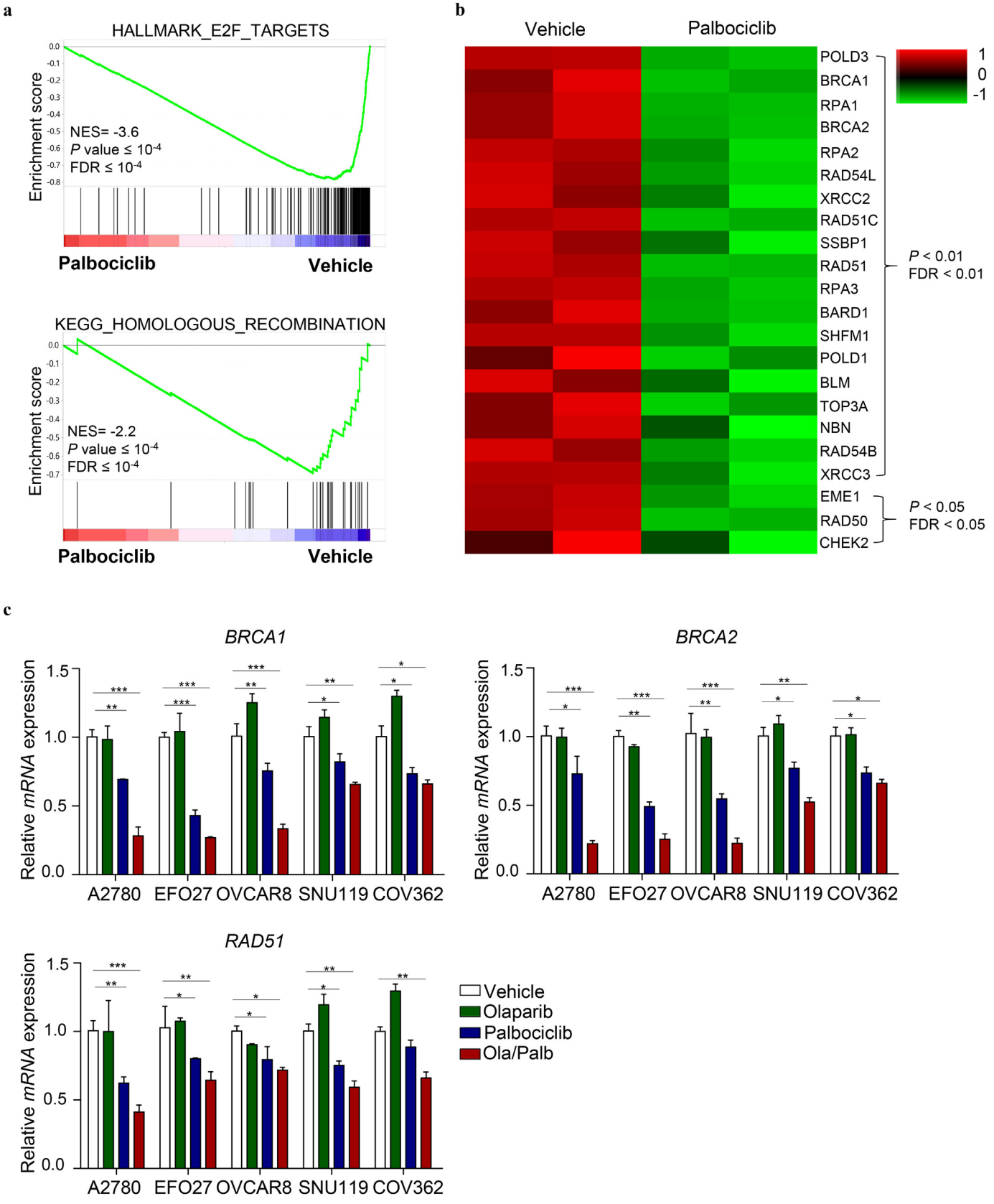


**Fig. 2.** CDK4/6 inhibition by Palbociclib results in downregulation of E2F targets and homologous recombination repair pathway genes. (a) GSEA of E2F and homologous recombination gene signatures in Palbociclib-treated A2780 cells *versus* control cells. Bars represent individual genes in a ranked data set list. NES, normalized enrichment score. (b) Heat map expression plot of 22 downregulated HR repair pathway genes in A2780 cells treated with vehicle or Palbociclib for 24 h. The gene expression was calculated according to the FPKM value. *P* value <0.05 and FDR < 0.05. (c) Quantitative reverse transcription PCR analysis of *BRCA1*, *BRCA2* and *RAD51* mRNA expression in ovarian cancer cells treated with drugs as indicated for 24 h. Mean ± S.D. for three independent experiments are shown. A2780, EFO27 and OVCAR8: Olaparib, 2 μM; Palbociclib, 1 μM. SNU119 and COV362: Olaparib, 8 μM; Palbociclib, 4 μM. Mean ± S.D. for three independent experiments are shown. $^{*}P < 0.05$; $^{**}P < 0.01$; $^{***}P < 0.001$ (Student's *t*-test).

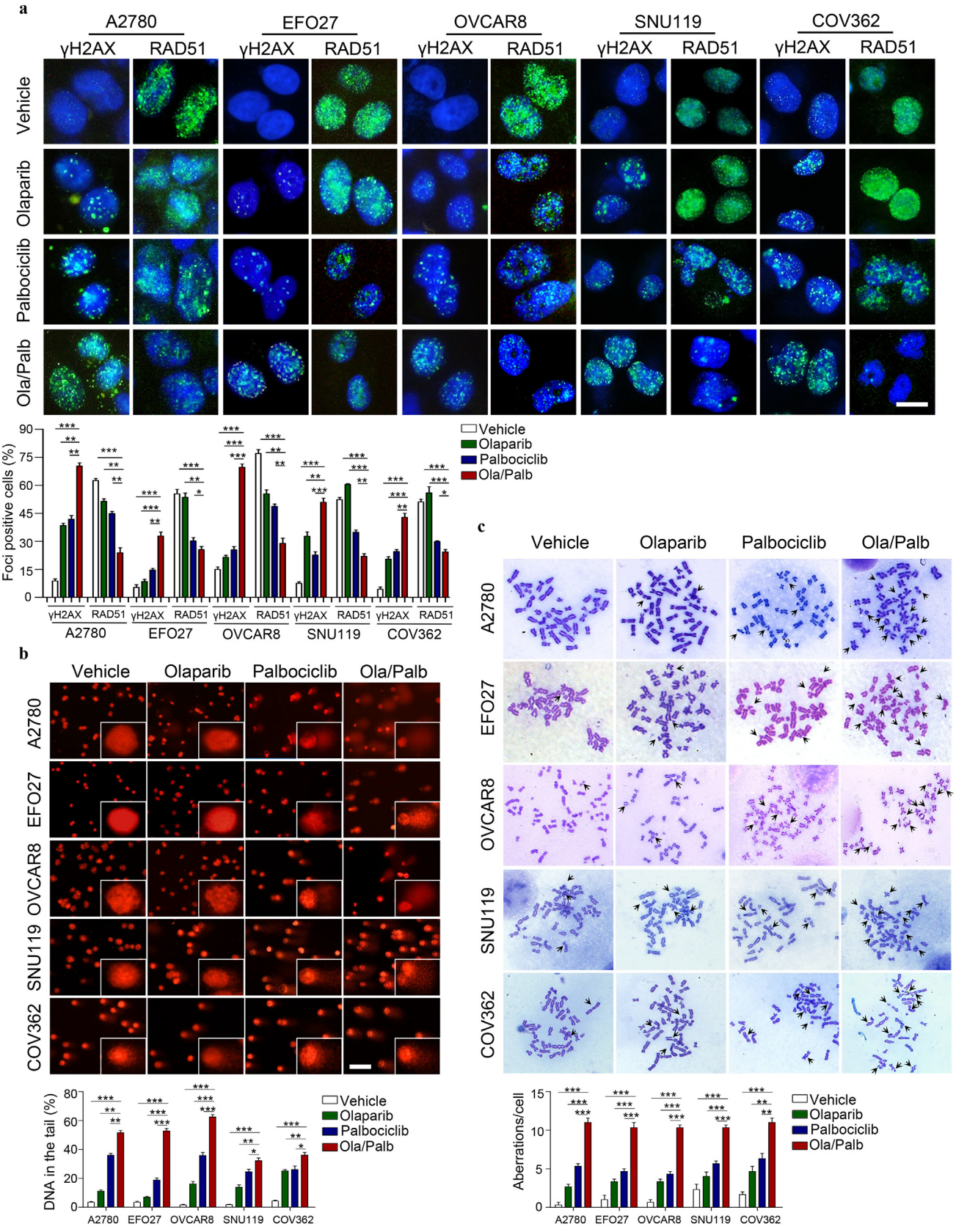


**Fig. 3.** The combination of Olaparib and Palbociclib results in reduced formation of RAD51 foci and induces DNA damage and chromosome instability in ovarian cancer cell lines. (a) Representative images of immunofluorescent staining of γH2AX and RAD51 in ovarian cancer cell lines treated with drugs as indicated for 48 h. Scale bar, 20 μm. Cells containing more than five foci were scored as positive. Means ± S.D. for three independent experiments are shown. (b) DNA damage was measured by comet assay in ovarian cancer cells (A2780, EFO27, OVCAR8, SNU119, and COV362) treated with drugs as indicated for 48 h. Scale bar, 50 μm. Quantification of DNA in the tail from three independent experiments is shown as mean ± S.D. (c) Metaphase spread analysis of chromosome aberrations in A2780, EFO27, OVCAR8, SNU119, and COV362 cells after drug treatment for 48 h. Mean ± S.D. for three independent experiments are shown. Representative metaphase spreads are shown. A2780, EFO27 and OVCAR8: Olaparib, 2 μM; Palbociclib, 1 μM. SNU119 and COV362: Olaparib, 8 μM; Palbociclib, 4 μM. $^{*}P < 0.05$; $^{**}P < 0.01$; $^{***}P < 0.001$ (Student's *t*-test).

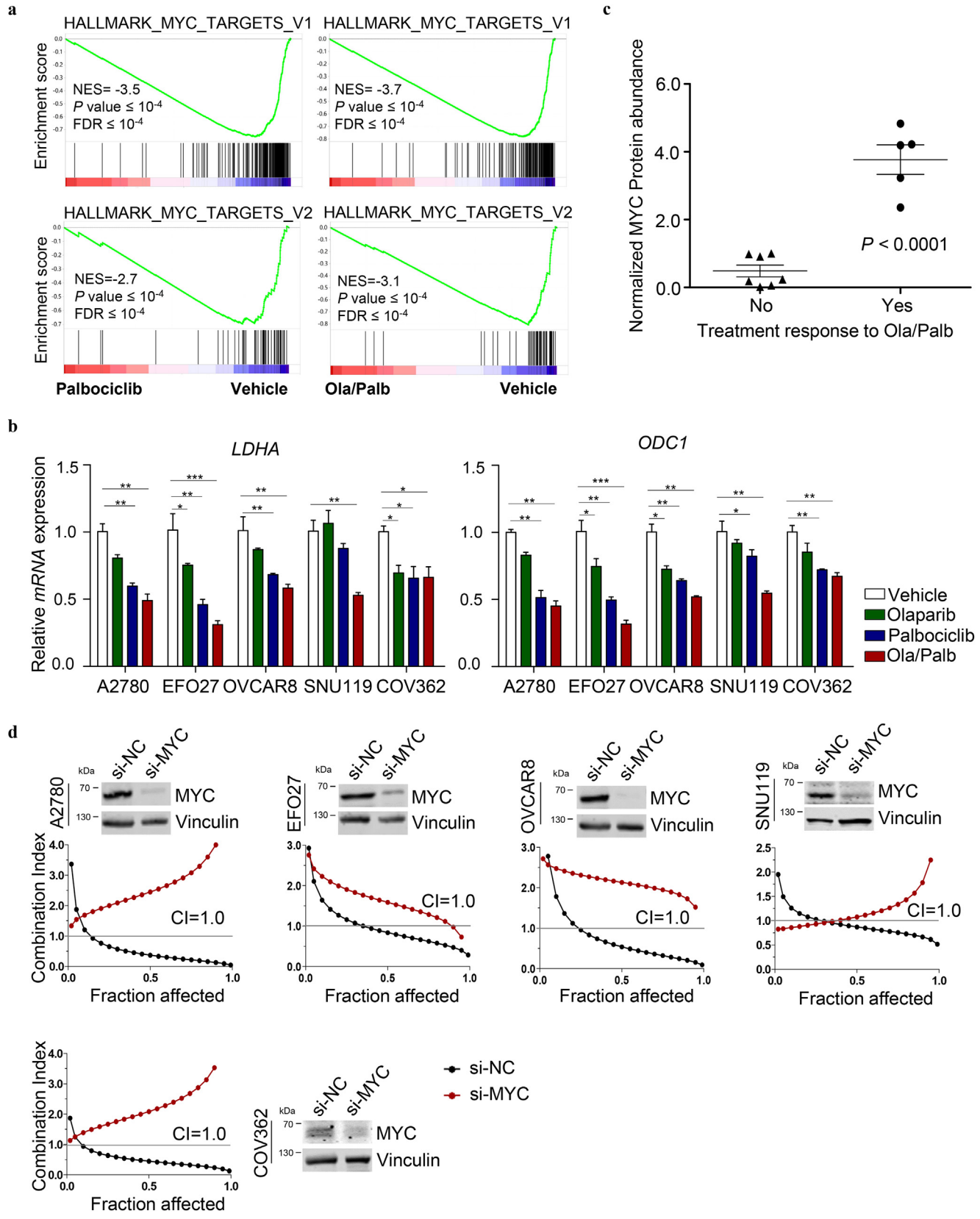


**Fig. 4.** CDK4/6 inhibition by Palbociclib results in downregulation of MYC targets, sensitizing ovarian cancer cells to PARP inhibition by Olaparib. (a) GSEA of MYC gene signatures in Palbociclib-treated (left panels) or Ola/Palb-treated (right panels) A2780 cells compared to Vehicle-treated cells. (b) Quantitative reverse transcription PCR analysis of *LDHA* and *ODC1* mRNA expression in A2780, EFO27, OVCAR8, SNU119, and COV362 ovarian cancer cell lines treated with drugs as indicated for 24 h. Mean ± S.D. for three independent experiments are shown. A2780, EFO27 and OVCAR8: Olaparib, 2 μM; Palbociclib, 1 μM. SNU119 and COV362: Olaparib, 8 μM; Palbociclib, 4 μM. (c) Normalized abundance of MYC protein in ovarian cancer cell lines that were grouped according to their treatment response to Olaparib and Palbociclib in combination (see Supplementary Fig. 6 for western blot analysis of MYC protein levels and Fig. 1 for treatment response data). (d) The synergistic effect of concomitant PARP and CDK4/6 inhibition in A2780, EFO27, OVCAR8, SNU119, and COV362 ovarian cancer cells was measured by cell viability assay after 72 h treatment. Western blot analysis of MYC protein levels in ovarian cancer cells with or without *MYC*-knockdown was shown. $^{*}P < 0.05$; $^{**}P < 0.01$; $^{***}P < 0.001$ (Student's *t*-test).

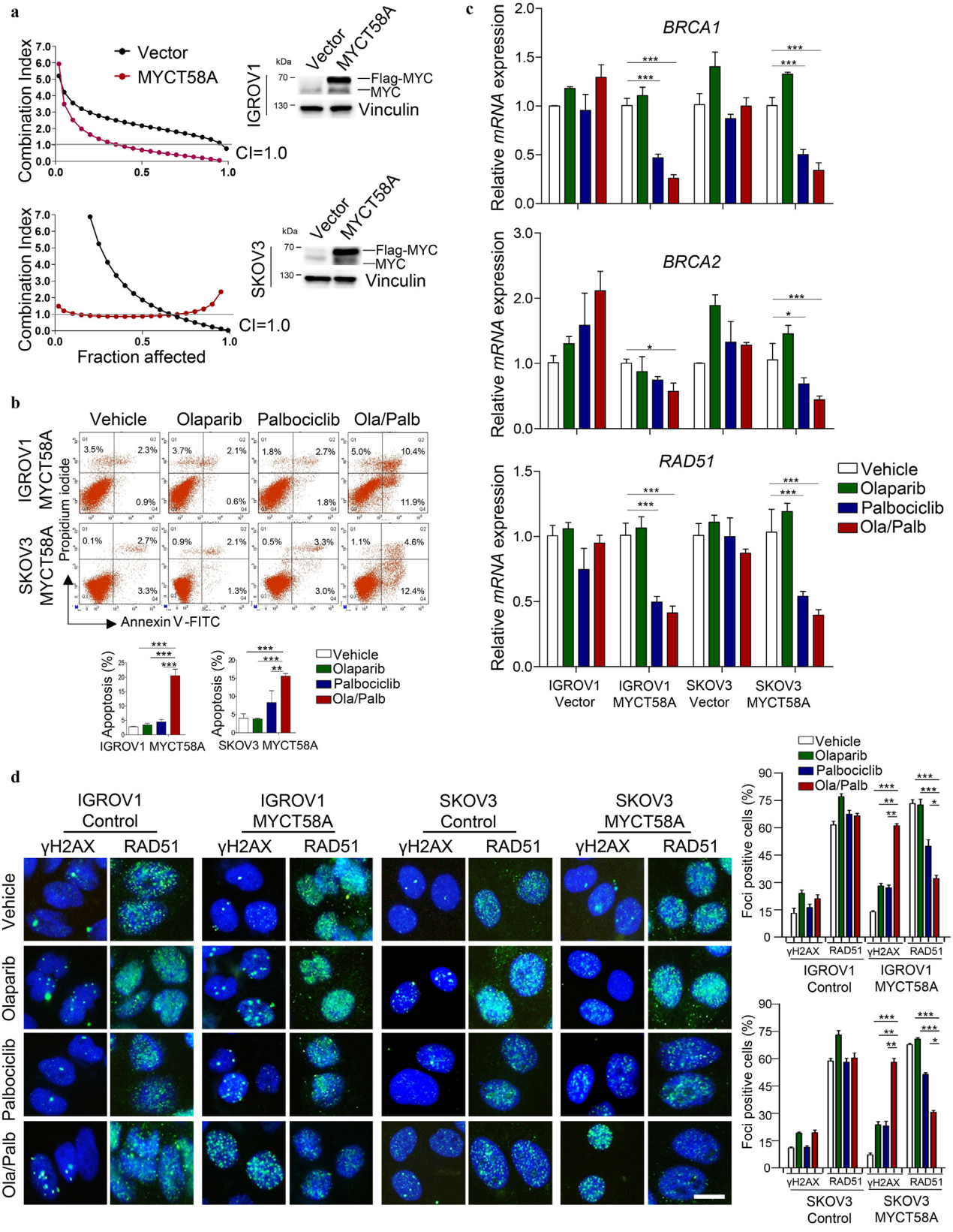


**Fig. 5.** Ectopic expression of MYC sensitizes ovarian cancer cell lines to the combination of Olaparib and Palbociclib. (a) The synergistic effect of Olaparib and Palbociclib in IGROV1 and SKOV3 ovarian cancer cell lines with or without *MYCT58A* overexpression was measured by cell viability assay after 72 h treatment. Western blot of MYC protein levels in cells as indicated. (b) Flow cytometric analysis of Annexin V and propidium iodide (PI) stained cells (IGROV1 and SKOV3 engineered with vector or MYCT58A overexpression, respectively) to evaluate apoptosis. (c) Quantitative reverse transcription PCR analysis of *BRCA1*, *BRCA2* and *RAD51* expression in ovarian cancer cell lines with or without MYCT58A overexpression, treated with drugs as indicated for 24 h. Mean ± S.D. for three independent experiments are shown. (d) Representative images of immunofluorescent staining of γH2AX and RAD51 in ovarian cancer cell lines treated with drugs as indicated for 48 h. Scale bar, 20 μm. Cells containing more than five foci were scored as positive. Mean ± S.D. for three independent experiments are shown. Olaparib, 2 μM; Palbociclib, 1 μM. $^{*}P < 0.05$; $^{**}P < 0.01$; $^{***}P < 0.001$ (Student's *t*-test).

of *BRCA1, BRCA2 and RAD51* to a varying degree (Supplementary Fig. 9). Collectively, these data suggest that CDK4/6i may induce HR repair deficiency through downregulation of MYC and its transcriptionally regulated HR repair pathway genes, causing synthetic lethality with Olaparib. Notably, however, as Palbociclib single-agent or in combination with Olaparib led to diminished phosphorylated Rb signals in all ovarian cancer cell lines examined regardless of treatment response (Supplementary Fig. 10a and b), inhibition of Rb phosphorylation was not sufficient to predict the synergistic activity of PARPi and CDK4/6i.

### 3.5. Combined use of Olaparib and Palbociclib is effective in vivo

We next evaluated the efficacy of Olaparib and Palbociclib in combination *in vivo*. The activity of the drug combination was examined using the xenograft mouse model of A2780 cells, an ovarian cancer cell line with high abundance of endogenous MYC protein (Fig. 4c and Supplementary Fig. 6). While single-agent Olaparib or Palbociclib had limited activity, the combination treatment significantly slowed down the tumor growth (Fig. 6a and b). As determined by the histological analysis, the combination treatment caused substantially reduced Ki67 (a proliferation marker) but increased Cleaved-Caspase 3 (an apoptosis marker) staining positive cells (Fig. 6c). Thus, decreased proliferation and increased apoptosis may, at least in part, explain for the objective treatment response to the combined PARPi-CDK4/6i. The target inhibition of CDK4/6 kinase activity *in vivo* was achieved as single-agent Palbociclib sufficiently suppressed Rb phosphorylation (Fig. 6c). In line with our *in vitro* results, CDK4/6 inhibition by Palbociclib resulted in markedly reduced MYC expression, and the addition of Olaparib led to nearly diminished MYC levels (Fig. 6c). Concordantly, combined use of Olaparib and Palbociclib resulted in a substantial increase in the formation of γH2AX nuclear foci and concomitantly a marked decrease in RAD51 positive foci (Fig. 6c). These results are thus consistent with our hypothesis that CDK4/6 inhibition is synthetic lethal with PARP inhibition through inducing downregulation of MYC expression and HR repair deficiency. Notably, although the drug combination failed to induce tumor regression, we did observe markedly reduced density of viable cells in tumors harvested at the end-point of the treatment from the combination group compared to either single-agent groups (Fig. 6d and e).

## 4. Discussion

While both PARPi and CDK4/6i have shown promising clinical benefits to their respective molecularly defined cancers, there is an urgent need to develop new combination therapies to improve treatment response and overcome emerging drug resistance. Many preclinical and clinical trials are underway investigating the therapeutic potential of combining PARP inhibitors with anti-angiogenic agents (*e.g.* Cediranib and Bevacizumab) [28,29], immunotherapies (*e.g.* antibodies to PD1/PD-L1 and CTLA-4) [30,31], and other targeted (*e.g.* PI3K, HSP90 and ATR inhibitors [32–37] or chemotherapeutic agents [6,38] (www.clinicaltrials.gov). In the current study, we demonstrate the therapeutic synergy between PARP inhibitor Olaparib and CDK4/6 inhibitor Palbociclib in ovarian cancer cells *in vitro* and *in vivo*, and identify MYC status as a predictor for response to PARPi and CDK4/6i in combination. Mechanistically, CDK4/6 inhibition by Palbociclib is synthetic lethal with PARP inhibition by Olaparib through inducing HR deficiency in a MYC-dependent manner.

CDK4/6 inhibitors have demonstrated therapeutic efficacy in CDK4/6-dependent tumors with $p16^{INK4a}$ loss or intact RB [19,39]. However, recent studies also indicate that neither intact RB function nor the presence of *CDKN2A* loss necessarily predicts CDK4/6 dependence [40]. As CDK4/6 inhibitor-based combination therapies have continued to emerge, it is imperative to identify biomarkers of response or determinants of sensitivity in the combinatorial treatment setting. In the current study, Palbociclib sufficiently suppresses RB phosphorylation in all cell lines examined despite the variable responses to the combination treatment. Thus, apparently, loss of RB activity induced by CDK4/6 inhibition is not sufficient to predict the treatment response to combined use of Palbociclib and Olaparib. Instead, our data indicate that CDK4/6 inhibition-induced downregulation of MYC and its target genes appears reliable for predicting the response to the synergistic effect of CDK4/6 and PARP inhibitors.

The role of MYC in DNA damage response and genomic instability has been a subject of debate and controversy [41–43]. Previous studies have reported that deregulation of MYC could induce DNA damage and genomic instability [41,42,44]. MYC has been shown to bind to the promoters of a number of DNA double strand-break (DSB) repair genes and transcriptionally regulate multiple components of the HR repair pathway [45–47], suggesting a functional relationship between MYC and HR activity. Concordantly, MYC-driven tumors, often with *MYC* amplification or high MYC protein abundance, are associated with increased DSB marker γH2AX foci and HR repair activity [44]. Consistent with these previous reports, our data also suggest that MYC may positively regulate the expression of a number of key HR repair pathway genes including *RAD51*, *BRCA1* and *BRCA2*. Nevertheless, there are also several reports indicating an inverse correlation between MYC transcriptional activity and DNA repair activity or chromosome stability [48–50]. While MYC appears to regulate DNA damage response and genome integrity in a context-dependent manner, some of these previous studies suggest that increased MYC expression may be associated with improved sensitivity to PARP inhibition through downregulating HR repair gene expression. In fact, our work highlights the critical role of MYC-mediated HR repair function in the synergistic response to combined PARPi-CDK4/6i in ovarian cancer.

Our data herein indicate that CDK4/6 positively regulates the oncogenic activity of MYC in a subset of ovarian cancer cells. However, the effects of CDK4/6 on the expression and activity of MYC in cancer have been controversial, and likely occur in a tissue-specific manner [51,52]. Our finding is concordant with a previous report that CDK4/6 mediates the proliferative and oncogenic activity of MYC in epithelial tissues [18]. Similarly, CDK4/6 inhibitor Ribociclib (LEE011) decreases the expression of E2F target genes including *MYC* and inhibits proliferation of aggressive thyroid cancer [51]. However, in contrast to the suppressing effect of CDK4/6 inhibition on MYC activity, works in HCT116 colon cancer cells have shown that siRNA-mediated CDK4/6 silencing results in an accumulation of MYC protein and its downstream network, a metabolic adaptive response of cancer cells to CDK4/6 inhibition [52]. While it remains to be investigated if CDK4/6i may regulate MYC in a tissue-specific manner, we provide evidence that Palbociclib induces downregulation of MYC and its target genes involved in HR repair, causing synthetic lethality with PARP inhibition in ovarian cancer cells.

High-grade serous ovarian carcinoma (HGSOC) is the most common histologic subtype of ovarian cancer. Due to significant tumor heterogeneity of HGSOC, it remains challenging to mimic and study such complex diseases using appropriate cancer cell line models. It has been reported by Domcke *et al* that a significant number of cancer cell lines commonly used (*e.g.* A2780 and SKOV3) in preclinical ovarian cancer research studies published to date exhibit molecular profiles very different from those of high-grade ovarian cancer patients samples [53]. Importantly, their work has identified several rarely used cell lines (*e.g.* OVCAR4, SNU119, and COV362) as the most suitable models of HGSOC. A recent more comprehensive cell line characterization study by Papp *et al* has confirmed the utility of these and other ovarian cancer cell lines for studying the disease at a preclinical level [54]. For example, EFO27 is a mucinous ovarian cancer cell line but it is high grade. IGROV1 contains a higher tumor mutational burden than commonly seen in ovarian cancer. In the current study, we used a diverse cell line panel of ovarian cancer to minimize cell line specific observations. The finding of this study may help extend the utility of the drug combination modality, *i.e.* Palbociclib plus Olaparib, to a broad spectrum of cancer types with similar genomic features with similar genomic features.

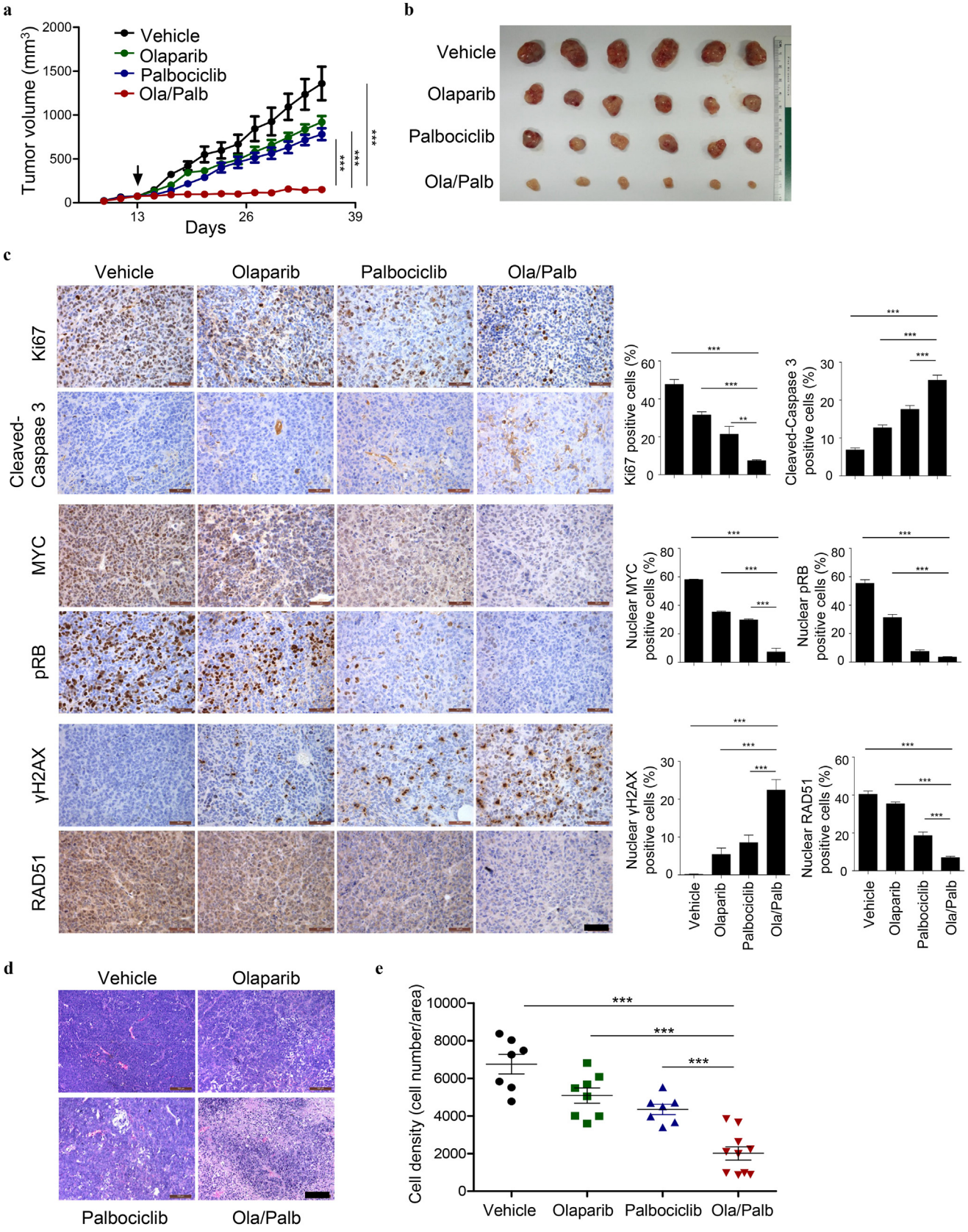


**Fig. 6.** Combined use of Olaparib and Palbociclib is effective *in vivo*. (a) Tumor growth curves of A2780 xenografted mice treated with Olaparib (50 mg/kg/day) and Palbociclib (125 mg/kg/day), either alone or in combination. The arrow indicates the treatment starting date. (b) Representative gross images of A2780 xenografted tumors isolated from mice in different treatment groups as indicated. (c) Representative images of immunohistochemical staining for proteins as indicated in A2780 xenografted tumors ($n = 6$ per treatment group) treated with Olaparib and Palbociclib either as single-agents or in combination for 4 days. Scale bar, 50 μm. (d) Representative images of H&*E*-stained A2780 xenografted tumors ($n = 7$–10 per treatment group) harvested at the end of the indicated treatments. Scale bar, 100 μm. (e) Quantification of cell density (number of tumor cells/area) of A2780 xenografts. Each symbol represents an individual tumor. Data are shown as the mean ± S.E.M. $^{**}P < 0.01$; $^{***}P < 0.001$ (one-way ANOVA with Tukey's multiple comparison test).

Ovarian cancers with high MYC levels are associated with poor prognosis and platinum resistance [55]. MYC amplification is present in up to 35% of HGSOC (*www.cbioportal.org*). Previous work using mouse models of autochthonous breast tumors has suggested that CDK4/6 inhibitors should not be used in combination with Carboplatin to treat tumors that depends on CDK4/6 activity for proliferation [40]. In the current study, we demonstrate the therapeutic synergy of Palbociclib and Olaparib in ovarian cancer cell lines featuring high-grade serous histology and harboring MYC amplification (SNU119 and COV362) [53]. Notably, the single-agent effects of Olaparib in these two cell lines requires higher drug concentrations than those other cell lines with high MYC levels (EFO27, OVCAR8, and A2780). However, consistent with our hypothesis, CDK4/6 inhibition by Palbociclib also induces homologous recombination deficiency through downregulation of MYC-regulated HR pathway genes, causing synthetic lethality with PARP inhibition in these HGSOC cell lines. Our finding may thus open a new avenue for the treatment of high-grade ovarian cancer patients with high MYC levels, including those carboplatin resistant cases.

A large number of early-stage clinical trials examining PARPi-based or CDK4/6i-based combination therapies are currently under way in a variety of human malignancies including ovarian cancer (www.clinicaltrials.gov). However, none of these early trials involves a combination of these two classes of inhibitors, likely due to a lack of reliable biomarkers that are predictive of therapeutic response. In the current study, we demonstrate the synergistic responses to combined PARPi-CDK4/6i depend on MYC expression status in ovarian cancer. Our finding is in line with a recent report showing therapeutic synergy between CDK1/2/5/9 inhibitor Dinaciclib-induced MYC blockade and PARP inhibitors in triple negative breast cancer models through downregulation of *RAD51* expression and induction of HR repair deficiency [45]. Collectively, our finding of MYC-dependent therapeutic synergy between PARP and CDK4/6 inhibitors may warrant clinical assessment with a potential to benefit patients whose tumors show high MYC expression and who do not respond to PARP inhibitors or CDK4/6 inhibitors monotherapy.

## Funding

This work was supported by the National Natural Science Foundation of China (No. 81672575, No. 81874111, No.81472447 to H Cheng; No. 81572586 and No. 81372853 to P Liu), the Liaoning Provincial Climbing Scholars Supporting Program of China (H Cheng, P Liu), the Liaoning Provincial Science and Technology Program for Oversea Talents (H Cheng), the Provincial Natural Science Foundation of Liaoning (No. 2014023002 to P Liu) and the Liaoning Provincial Key Basic Research Program for Colleges and Universities (LZ2017002 to H Cheng). None of these funding sources had any role in writing the manuscript nor the decision to submit for publication.

## Author contributions

H.C., P.L. and J.Y. conceived and designed the study, and wrote the manuscript. J.Y. and C.L performed major experiments, collected, and analyzed data. Y.J., X.S., M.W., K.J., F.L., L.S. and Y.X., performed flow cytometry analysis and quantitative RT-PCR assay. Z.T. conducted GSEA analysis. All authors contributed and approved the manuscript.

## Conflict of interest

The authors declare that they have no conflicts of interest.

## Ethics statement

All animal procedures were conducted under the approval of the Animal Care and Use Committee of Dalian Medical University.

## Acknowledgments

We thank members of Dalian Key Laboratory of Molecular Targeted Caner Therapy and the Liu Laboratory for discussions throughout the study.

## Appendix A. Supplementary data

Supplementary data to this article can be found online at https://doi.org/10.1016/j.ebiom.2019.03.027.

## References

[1] Matulonis U, Sood A, Fallowfield L, Howitt B, Sehouli J, Karlan B. Ovarian cancer. Nat Rev Dis Primers 2016;2:16061.
[2] Jemal A, Siegel R, Xu J, Ward E. Cancer statistics. CA Cancer J Clin 2011;61(2):69–90.
[3] Siegel RL, Miller KD, Jemal A. Cancer statistics, 2016. CA Cancer J Clin 2010;60(5):277–300.
[4] Bookman MA, Brady MF, McGuire WP, et al. Evaluation of new platinum-based treatment regimens in advanced-stage ovarian cancer: a phase III trial of the gynecologic Cancer intergroup. J Clin Oncol 2009;27(9):1419–25.
[5] Bowtell DD, Böhm S, Ahmed AA, et al. Rethinking ovarian cancer II: reducing mortality from high-grade serous ovarian cancer. Nat Rev Cancer 2015;15(11):668–79.
[6] Lord CJ, Ashworth A. PARP inhibitors: synthetic lethality in the clinic. Science 2017;355(6330):1152–8.
[7] Vaughan S, Coward JI, et al. Rethinking ovarian cancer: recommendations for improving outcomes. Nat Rev Cancer 2011;11(10):719–25.
[8] TCGA. Cancer genome atlas research network: integrated genomic analyses of ovarian carcinoma. Nature 2011;474:609–15.
[9] Konstantinopoulos PA, Ceccaldi R, Shapiro GI, D'Andrea AD. Homologous recombination deficiency: exploiting the fundamental vulnerability of ovarian Cancer. Cancer Discov 2015;5(11):1137–54.
[10] Scott CL, Swisher EM, Kaufmann SH. Poly (ADP-ribose) polymerase inhibitors: recent advances and future development. J Clin Oncol Off J Am Soc Clin Oncol 2015;33(12):1397–406.
[11] Nc T. Inhibition of poly(ADP-ribose) polymerase in tumors from BRCA mutation carriers. New England J Med 2009;361(17):123–34.
[12] Lord CJ, Ashworth A. BRCAness revisited. Nat Rev Cancer 2016;16(2):110.
[13] Lord CJ, Tutt ANJ, Ashworth A. Synthetic lethality and Cancer therapy: lessons learned from the development of PARP inhibitors. Annu Rev Med 2015;66(1):455–70.
[14] Gelmon KA, Tischkowitz M, Mackay H, et al. Olaparib in patients with recurrent high-grade serous or poorly differentiated ovarian carcinoma or triple-negative breast cancer: a phase 2, multicentre, open-label, non-randomised study. Lancet Oncol 2011;12(9):852–61.
[15] Mirza MR, Monk BJ, Herrstedt J, et al. Niraparib maintenance therapy in platinum-sensitive, recurrent ovarian Cancer. N Engl J Med 2016;375(22):2154–64.
[16] ME K, M K, LE D, WD T, A K. CDK4/6 inhibitors: the mechanism of action May not be as simple as once thought. Cancer Cell 2018;34(1):9–20.
[17] Ma CX, Gao F, Luo J, et al. NeoPalAna: neoadjuvant palbociclib, a cyclin-dependent kinase 4/6 inhibitor, and anastrozole for clinical stage 2 or 3 estrogen receptor positive breast cancer. Clin Cancer Res 2017;23(15):4055–65.
[18] Asghar U, Witkiewicz AK, Turner NC, Knudsen ES. The history and future of targeting cyclin-dependent kinases in cancer therapy. Nat Rev Drug Discov 2015;14(2):130–46.
[19] O'Leary B, Finn RS, Turner NC. Treating cancer with selective CDK4/6 inhibitors. Nat Rev Clin Oncol 2016;13(7):417.
[20] Ashton JC. Drug combination studies and their synergy quantification using the Chou-Talalay method–letter. Cancer Res 2015;75(11):2400.
[21] Muranen T, Selfors LM, Worster DT, et al. Inhibition of PI3K/mTOR leads to adaptive resistance in matrix-attached cancer cells. Cancer Cell 2012;21(2):227–39.
[22] Speit G, Hartmann A. The comet assay: a sensitive genotoxicity test for the detection of DNA damage and repair. Methods Mol Biol 2006;314:275.
[23] Gudmundsdottir K, Lord CJ, Witt E, Tutt ANJ, Ashworth A. DSS1 is required for RAD51 focus formation and genomic stability in mammalian cells. EMBO Rep 2004;5(10):989–93.
[24] Singh M, Mukundan S, Jaramillo M, Oesterreich S, Sant S. Three-dimensional breast Cancer models mimic hallmarks of size-induced tumor progression. Cancer Res 2016;76(13):3732–43.
[25] Shim H, Dolde C, Lewis BC, et al. C-Myc transactivation of LDH-A: implications for tumor metabolism and growth. Proc Natl Acad Sci U S A 1997;94(13):6658.
[26] Hogarty MD, Norris MD, Davis K, et al. ODC1 is a critical determinant of MYCN oncogenesis and a therapeutic target in neuroblastoma. Cancer Res 2008;68(23):9735.
[27] Yeh E, Cunningham M, Arnold H, et al. A signalling pathway controlling c-Myc degradation that impacts oncogenic transformation of human cells. Nat Cell Biol 2004;6(4):308–18.
[28] Dean E, Middleton MR, Pwint T, et al. Phase I study to assess the safety and tolerability of olaparib in combination with bevacizumab in patients with advanced solid tumours. Br J Cancer 2012;106(3):468–74.
[29] Ivy SP, Liu JF, Lee JM, Matulonis UA, Kohn EC. Cediranib, a pan-VEGFR inhibitor, and olaparib, a PARP inhibitor, in combination therapy for high grade serous ovarian cancer. Expert Opin Investig Drugs 2016;25(5):597.

[30] Brown JS, Sundar R, Lopez J. Combining DNA damaging therapeutics with immunotherapy: more haste, less speed. Br J Cancer 2017;118(3):312–24.
[31] Higuchi T, Flies DB, Marjon NA, et al. CTLA-4 blockade synergizes therapeutically with PARP inhibition in BRCA1-deficient ovarian Cancer. Cancer Immunol Res 2015;3(11):1257.
[32] Ibrahim YH, Garcíagarcía C, Serra V, et al. PI3K inhibition impairs BRCA1/2 expression and sensitizes BRCA-proficient triple-negative breast Cancer to PARP inhibition. Cancer Discov 2012;2(11):1036.
[33] Juvekar A, Burga LN, Hu H, et al. Combining a PI3K inhibitor with a PARP inhibitor provides an effective therapy for BRCA1-related breast cancer. Cancer Discov 2012;2(11):1048.
[34] Bian X, Gao J, Luo F, et al. PTEN deficiency sensitizes endometrioid endometrial cancer to compound PARP-PI3K inhibition but not PARP inhibition as monotherapy. Oncogene 2018;37(3):341–51.
[35] Dong W, Min W, Nan J, et al. Effective use of PI3K inhibitor BKM120 and PARP inhibitor Olaparib to treat PIK3CA mutant ovarian cancer. Oncotarget 2016;7(11):13153.
[36] Choi YE, Battelli C, Watson J, et al. Sublethal concentrations of 17-AAG suppress homologous recombination DNA repair and enhance sensitivity to carboplatin and olaparib in HR proficient ovarian cancer cells. Oncotarget 2014;5(9):2678–87.
[37] Kim H, George E, Ragland RL, et al. Targeting the ATR/CHK1 Axis with PARP inhibition results in tumor regression in BRCA-mutant ovarian Cancer models. Gynecol Oncol 2017;145(12):3097.
[38] Dréan A, Lord CJ, Ashworth A. PARP inhibitor combination therapy. Crit Rev Oncol 2016;108:73–85.
[39] Konecny GE, Winterhoff B, Kolarova T, et al. Expression of p16 and retinoblastoma determines response to CDK4/6 inhibition in ovarian cancer. Clin Cancer Res 2011;17(6):1591–602.
[40] Roberts PJ, Bisi JE, Strum JC, et al. Multiple roles of cyclin-dependent kinase 4/6 inhibitors in cancer therapy. J Natl Cancer Inst 2012;104(6):476–87.
[41] Vafa O, Wade M, Kern S, et al. c-Myc can induce DNA damage, increase reactive oxygen species, and mitigate p53 function: a mechanism for oncogene-induced genetic instability. Mol Cell 2002;9(5):1031–44.
[42] Wade M, Wahl GM. c-Myc, genome instability, and tumorigenesis: The devil is in the details. Springer Berlin Heidelberg; 2006.
[43] Prochownik EV, Li Y. The ever expanding role for c-Myc in promoting genomic instability. Cell Cycle 2007;6(9):1024–9.
[44] Meyer N, Penn LZ. Reflecting on 25 years with MYC. Nat Rev Cancer 2008;8(12):976–90.
[45] Carey JP, Karakas C, Bui T, et al. Synthetic lethality of PARP inhibitors in combination with MYC blockade is independent of BRCA status in triple negative breast cancer. Cancer Res 2017;78(3).
[46] Ambrosio S, Amente S, Napolitano G, Di PG, Lania L, Majello B. MYC impairs resolution of site-specific DNA double-strand breaks repair. Mutat Res 2015;774:6.
[47] Chen Y, Xu J, Borowicz S, Collins C, Huo D, Olopade OI. c-Myc activates BRCA1 gene expression through distal promoter elements in breast cancer cells. BMC Cancer 2011;11:246.
[48] Jin Z, May WS, Gao F, Flagg T, Deng X. Bcl2 suppresses DNA repair by enhancing c-Myc transcriptional activity. J Biol Chem 2006;281(20):14446–56.
[49] Song L, Dai T, Xie Y, et al. Up-regulation of miR-1245 by c-myc targets BRCA2 and impairs DNA repair. J Mol Cell Biol 2012;4(2):108–17.
[50] Li Z, Owonikoko TK, Sun S-Y, et al. c-Myc suppression of DNA double-strand break repair 1 2. Neoplasia 2012;14(12) [1190,IN32-202,IN35].
[51] Lee HJ, Lee WK, Kang CW, Ku CR, Cho YH, Lee EJ. A selective cyclin-dependent kinase 4, 6 dual inhibitor, Ribociclib (LEE011) inhibits cell proliferation and induces apoptosis in aggressive thyroid cancer. Cancer Lett 2018;417:131–40.
[52] Tarrado-Castellarnau M, De Atauri P, Tarrago-Celada J, et al. De novo MYC addiction as an adaptive response of cancer cells to CDK4/6 inhibition. Mol Syst Biol 2017;13(10):940.
[53] Domcke S, Sinha R, Levine DA, Sander C, Schultz N. Evaluating cell lines as tumour models by comparison of genomic profiles. Nat Commun 2013;4:2126.
[54] Papp E, Hallberg D, Konecny GE, et al. Integrated genomic, Epigenomic, and expression analyses of ovarian Cancer cell lines. Cell Rep 2018;25(9):2617–33.
[55] Reyes-Gonzalez JM, Armaiz-Pena GN, Mangala LS, et al. Targeting c-MYC in platinum-resistant ovarian Cancer. Mol Cancer Ther 2015;14(10):2260–9.